Made available by Hasselt University Library in https://documentserver.uhasselt.be

Why and how to adapt PID testing for bifacial PV modules?

Peer-reviewed author version

CAROLUS, Jorne; BREUGELMANS, Robbe; Tsanakas, John; VAN DER HEIDE, Arvid; Voroshazi, Eszter; DE CEUNINCK, Ward & DAENEN, Michael (2020) Why and how to adapt PID testing for bifacial PV modules?. In: Progress in Photovoltaics, 28 (10), p. 1045-1053.

DOI: 10.1002/pip.3311
Handle: http://hdl.handle.net/1942/31480

PROGRESS IN PHOTOVOLTAICS

Why and how to adapt PID testing for bifacial PV modules?

Journal:	*Progress in Photovoltaics: Research and Applications*
Manuscript ID	PIP-20-012.R2
Wiley - Manuscript type:	Research Article
Date Submitted by the Author:	n/a
Complete List of Authors:	Carolus, Jorne; Breugelmans, Robbe; Hasselt University; IMEC Tsanakas, John; IMEC, Department of Photovoltaics van der Heide, Arvid; IMEC, Department of Photovoltaics Voroshazi, Eszter; imec, PV De Ceuninck, Ward; IMEC; Hasselt University Daenen, Michael; Hasselt University; IMEC
Keywords:	Crystalline silicon solar cells, n-PERT bifacial solar cells, photovoltaic (PV) module reliability, potential-induced degradation (PID), testing methods

SCHOLARONE™
Manuscripts

Why and how to adapt PID testing for bifacial PV modules?

Jorne Carolus[1,2,a], Robbe Breugelmans[1,2], John A. Tsanakas[2], Arvid van der Heide[2], Eszter Voroshazi[2], Ward De Ceuninck[1,2], Michaël Daenen[1,2]

[1] Hasselt University (partner in EnergyVille), Thor Park 8320, 3600 Genk, Belgium

[2] imec (partner in EnergyVille), Thor Park 8320, 3600 Genk, Belgium

Corresponding authors:

a) jorne.carolus@uhasselt.be

For Peer Review

Abstract - Recent research has shown that bifacial PV modules with a glass/glass packaging are prone to different PID mechanisms occurring simultaneously on the front and the rear side of the solar cell. With this in mind, researchers investigating the impact of PID on each side of the bifacial solar cell separately apply PID stress to one side of bifacial PV modules according to stress method (b) as described in the IEC TS 62804-1, i.e. contacting the surface with a conductive electrode. Yet, in this paper, we show that such practice of PID testing might result in an unintended development of an electric field between the environmental chamber and the non-stressed side of the solar cell. Through our experimental study we reveal that this electric field results in unintended bifacial PID stress of bifacial solar cells; which goes along with misleading interpretations of the evolving PID mechanisms and susceptibility of bifacial PV modules. Next to the methodology concerns, we discuss three possible solutions to prevent such unintended PID mechanisms from occurring.

Index Terms – Crystalline silicon solar cells, n-PERT bifacial solar cells, photovoltaic (PV) module reliability, potential-induced degradation (PID), testing methods

For Peer Review

1. Introduction

Bifacial crystalline silicon (c-Si) PV technology has long been considered as a novelty and rather a niche with, until recently, minor uptake in the PV market and end-use share[1]. Yet, following the recent shift towards mass production of advanced cell technologies (i.e. PERC, PERT and heterojunction), and the shift towards glass/glass (GG) modules, bifacial PV modules are finally becoming a commercial reality and enter the mainstream.[1-4]

Towards broader adoption of bifacial PV in large scale, further R&D effort is required to address the needs for: i) better predictability of bifacial PV energy yield in real-field conditions and ii) tailored characterization and reliability testing, i.e. for optimal performance and reliability of bifacial PV modules. Focusing on the latter, recent research efforts have pointed out potentially dominant reliability issues (i.e. degradation/failure modes) specific to both bifacial PV modules and bifacial PV installations. Besides, while power degradation occurs on both sides of a bifacial PV module, it contributes differently to the overall performance losses of the module[5,6]. Thereon, such reliability issues impose additional and/or updated considerations for new characterization and reliability testing sequences. In particular, design-for-reliability for bifacial PV modules should address their intrinsically higher operational currents, the use of double glass (front and back cover) layouts or novel transparent sheet materials, as well as the trend towards higher operational voltages[7-10]. On this basis, it is recommended today not only to check for an approved IEC 61215 test on the bifacial PV module type considered for use, but also for additional tests, e.g. for PID (IEC TS 62804-series) and junction boxes/bypass diodes (IEC 62979, IEC TS 62916).

Especially PID has been shown to trigger significant reliability risks and rapid power losses in bifacial PV modules and systems [11-15]; therefore, it is considered among the most critical failure modes with a high impact on energy yield and financial losses[16]. In typical stress tests for PID, a high voltage between the solar cell matrix and the frame of the module is applied. For such tests, the module terminals are short-circuited, rendering a uniform potential across the solar cells; while the environmental stressors can be either applied in indoor (controlled) set-ups (accelerated testing) or in outdoor (real-field) conditions. In principle, at the system level, the severity of PID is a superlinear function of the applied (operational) voltage on the affected PV module or string [5,17,18]; while, at material level, it is significantly enhanced by the low volume resistivity of the encapsulation material and glass cover [19]. Until now, research has identified three different PID modes for bifacial c-Si solar cells, namely PID of the shunting type (PID-s), PID of the polarization type (PID-p), and PID of the corrosive type (PID-c) [20-23]. PID-s has been shown to be caused by sodium (Na) diffusing into silicon stacking faults through the pn-junction, and thus shunting the cell [20,24-26]. This degradation mode affects primarily the fill factor (FF), next the open-circuit voltage (V_{OC}), and lastly the short-circuit current (I_{SC}) [27,28]. PID-p on the other hand is described as a temporary and reversible degradation of the passivation layer, which reduces the performance due to a surface recombination increase [21,29-31]. PID-p can be identified by a significant loss in I_{SC} and V_{OC} while the FF remains unaffected. For one of the PID-c mechanisms observed in bifacial solar cells, it is assumed that beneath the AlO_X/SiN_Y passivation layer stack a corrosion process of the Si surface occurs, resulting in the formation of a SiO_2 layer [23]. It has been shown that this degradation mode only affects I_{SC} and V_{OC} similarly to the behaviour under PID-p. However, PID-c shows an irreversible behaviour whereas PID-s and PID-p are shown to be reversible with thermal treatment and/or the application of reverse bias between the active cell circuit and the grounded module frame [21,23,32]. In addition, degradation due to PID-p has been shown to be recoverable by light, which might slow down or even mitigate the degradation process in the field.[21,23,33]

Thoroughly understanding the physics and the underlying electrical/thermal/optical "signatures" of such PID mechanisms (both theoretically and experimentally) is of key importance for defining sufficient and suitable reliability testing, as well as best practices for characterization and optimal material selection for PV module components and cell technology. Particularly bifacial PV modules have been proven susceptible to the aforementioned PID mechanisms, which might occur in isolation or in combination on both the front and the rear side of the cell/module [22,23]. PV module manufacturers, at the final stage of product certification, are mostly interested in PID qualification tests and mainly perform the experiments according to stress method (a) as described in IEC TS 62804-1[34], i.e. testing in damp heat using an environmental chamber, which results in bifacial PID stress with an inhomogeneous electric field distribution over the front and rear covers of the (bifacial) PV module. Alternatively, in the early stage of the cell and/or module material development, quantitative testing is implemented according to stress method (b) as described in the IEC TS 62804-1, i.e. contacting the surface with a conductive electrode, hereafter referred to as foil-method. This results in a twofold advantage: i) it allows the researchers to apply monofacial PID stress on bifacial PV modules

For Peer Review

by applying the foil at only one side of the PV module and ii) it allows a homogeneous electric field distribution of the full area of the PV cell/module. However, by implementing this approach, unexpected results have emerged when bifacial PV modules were subjected to monofacial PID stress.[35] In this context it has been shown that bifacial n-PERT solar cells under rear-side monofacial PID stress show the same degradation behaviour as under front-side monofacial PID stress and the authors concluded that the degradation mechanism is the same and that the stressing side is of minor importance.

With this work, we show that one must take additional measures and follow a certain approach to individually reveal and investigate the effect and propagation of PID on each side of a bifacial solar cell. We focus on the PID testing methodology and the impact of the approach on the test results. This was obtained by subjecting single-cell laminates with identical bifacial solar cells to a PID test using four different test setups. Details of the different test setups are described in the following section. Interestingly, this renewed approach uncovered a significant difference between front- and rear-side monofacial PID stress of such n-PERT solar cells, and therefore highlights the importance of using a correct methodology when PID stressing bifacial solar cells[36,37].

2. Experimental

A. Sample preparation

Eight identical bifacial front junction (FJ) mono c-Si n-PERT solar cells of 156 mm x 156 mm were laminated into eight frameless single-cell PV laminates of 200 mm x 200 mm using a PID prone, commercially available encapsulant, hereafter referred to as single-cell laminates. Six out of the eight laminates were manufactured using a 3 mm soda lime glass (SLG) glass/glass (GG) configuration (configuration A) while the two remaining laminates were made using a transparent frontsheet and a 3 mm SLG at the rear side (configuration B). All single cell laminates were produced at imec's EnergyVille module lab with the same lamination recipe. The initial efficiency (η), I_{SC}, V_{OC} and FF of the eight single-cell laminates, characterized under both front- and rear-side illumination measurements, are shown in Table 1.

In order to exclude degradation mechanisms other than PID, a GG reference sample, identical with the samples in configuration A, was included in this test. This sample was not put under high voltage stress and did not show any degradation during the experiments (results not included in this report).

B. PID Testing and Characterization

The single cell laminates underwent PID stress testing according to the foil-method as described in IEC TS 62804-1: "Test methods for detection of potential-induced degradation of crystalline silicon photovoltaic (PV) modules".[34] The foil-method was applied, with a temperature of 60°C and relative humidity of less than 60% being the (controlled, stable) environmental stress conditions throughout the test duration. A 1000 V potential difference was applied between the aluminium (Al) foils and the

For Peer Review

short-circuited solar cell. During PID stress, the solar cell was at a negative potential (-1000 V) to the Al foils (0 V). Hence, driving positive charges into the solar cell. Two laminates in configuration A were put under bifacial PID stress, i.e. Al foils attached to both the front and the rear SLG covers, which is shown in Figure 1a. Two laminates in configuration A underwent rear-side monofacial PID stress, i.e. Al foils attached to the rear SLG cover only, as shown in Figure 1b. The two laminates in configuration B were subjected to rear-side monofacial PID stress, which is shown in Figure 1c. The two remaining laminates in configuration A underwent rear-side monofacial PID stress while shielding the front side, i.e. Al foils attached to the front SLG cover while short-circuited with the solar cell and thus no electrical field existed between the front SLG and the solar cell, Figure 1d.

Intermediate measurements were performed regularly and the PV performance loss under PID stress was quantified using a pv-tools LOANA PV analysis system for all measurement methods. Next to light IV measurements at standard test conditions (STC), external quantum efficiency (EQE) measurements were also performed. All characterization measurements were conducted on both the front side and the rear side of the single-cell laminates using monofacial illumination and a black cloth underneath the laminate to reduce the reflected irradiance.

3. Results

A. *Bifacial PID stress in configuration A samples*

Two identical laminates in configuration A underwent bifacial PID stress testing to investigate the impact of PID on both sides of the FJ bifacial n-PERT solar cells. This setup is shown in Figure 1a. Front-side light IV measurements were conducted regularly during the PID stress test and the generated power output (P_{MAX}) degradation due to PID is shown in Figure 2. The graph shows that 721 hours of PID stress resulted in a P_{MAX} degradation level of 21% and 19% for sample one and sample two respectively. Under rear-side illumination measurements, we observed a 12% and 10% P_{MAX} degradation for both modules. Notably, more than 85% of the degradation occurred within the first 15 hours of PID stress. From Figure 2, it is also clear that under front-side illumination, PID is more present than under rear-side illumination. Both a higher degradation level as well as a higher degradation rate in the first couple of hours can be observed.

The light I-V curves of the front and the rear-side illumination measurements of the first laminate in configuration A before and after PID stress are shown in Figure 3a. The 21% P_{MAX} degradation under front-side illumination after 721 hours of bifacial PID stress originates from losses in I_{SC} (~10%), V_{OC} (~7%), and FF (~3%) while under rear-side illumination, the 12% P_{MAX} degradation was attributed to losses originating from V_{OC} (~7%) and FF (~4%) whereas the change in I_{SC} was negligible. The second laminate in configuration A shows an almost identical behaviour for both the front and the rear-side illumination measurements: a P_{MAX} degradation of 19% with losses originating from I_{SC} (~9%), V_{OC} (~8%), and FF (~5%) at the front-side

For Peer Review

and a P_{MAX} degradation of 10%, originating from V_{OC} (~7%) and FF (~6%) at the rear side. This sample also showed a negligible change in I_{SC} under rear illumination, which is following the observations of the first sample. It should be noted that this degradation mechanism evolves very quickly and most of the damage is already done after only 15 hours of high voltage stress. The slight degradation which is observed after 15 hours of PID stress is attributed to a slow and almost linear decrease in FF.

Figure 3b. shows the EQE measurements of both the front and the rear side of the first laminate in configuration A under bifacial PID stress. The EQE measurements under front-side illumination of the single-cell laminate show a significant relative decrease in EQE response in the short- and mid-wavelength region (300–800 nm), whereas the long-wavelength region (800–1200 nm) remained unaffected during PID stress. On the contrary, rear-side EQE measurements do not show any change after 721 hours of PID stress. Indeed, the EQE measurements confirm that the degradation is due to a degradation mechanism evolving at the front-side of the solar cell. Furthermore, the limited decrease of the FF in combination with the EQE data proves that the underlying degradation mechanism is not caused by PID-s.

B. Rear-side PID stress in configuration A samples

From the previous section, we learned that the degradation mechanism of FJ bifacial n-PERT solar cells under bifacial PID stress is mainly occurring at the front side of the solar cell. However, this does not mean that the rear side is PID-free since the mechanism occurring at the front-side of the solar might outweigh the mechanism occurring at the rear side of the solar cell. Therefore, two identical laminates in configuration A underwent monofacial (rear-side) PID stress testing to investigate the impact of PID only on the rear side of their solar cell, as shown in Figure 1b. Front-side light IV measurements indicated a P_{MAX} degradation level of 17% and 18% for sample one and sample two respectively after over 150 hours of PID stress, whereas rear-side light I-V measurements show a 9% and 8% P_{MAX} degradation respectively (Figure 4). Remarkably, the results show a similar trend to the case where identical laminates underwent bifacial PID stress testing, i.e. PID-induced losses in power output are more evident under front-side illumination PID than under rear-side illumination, even under rear-side monofacial PID stress. Also, a higher degradation level, as well as a higher degradation rate in the first couple of hours under front-side illumination, can be observed. It can be seen that the mechanism under rear-side monofacial PID stress develops a PID outcome significantly more slowly than under bifacial PID stress. Eventually both stress tests lead to nearly the same level of degradation, but it took up to five times as long in the monofacial rear side test.

The light I-V curves obtained under front-side illumination measurements of the first laminate in configuration A during rear-side monofacial PID stress are shown in Figure 5a. The P_{MAX} degradation of 17% originates from losses in I_{SC} (~9%) and V_{OC} (~7%) while the fill factor remained unchanged. Under rear-side illumination measurements, a P_{MAX} degradation of 9% originating from V_{OC} (~7%) and FF (~2%) was observed while the change in I_{SC} was negligible. The second laminate in

For Peer Review

configuration A shows an almost identical behaviour for both the front and rear-side illumination measurements: an 18% P_{MAX} degradation originating from losses in I_{SC} (~10%), V_{OC} (~7%), and FF (~2%) and under rear-side illumination an 8% P_{MAX} degradation was attributed to losses originating from V_{OC} (~6%) and FF (~2%). This sample also showed a negligible change in I_{SC} under rear illumination, which is following the observations of the first sample.

Figure 5b. shows the EQE measurements of the front side of the first laminate in configuration A. The EQE measurements of the front side of the single-cell laminate show a significant relative decrease in EQE response in the short- and mid-wavelength region (300–800 nm), whereas the long-wavelength region (800–1200 nm) remained unaffected during PID stress. This is following the findings under bifacial stress of the identical samples in configuration A. It should be noted that the intermediately obtained EQE responses clearly show a slower PID behaviour than under bifacial PID stress. Rear-side EQE measurements do not show any change after 152 hours of PID stress. Indeed, the EQE measurements confirm that also under rear-side monofacial PID stress the degradation is due to a degradation mechanism evolving at the front side of the solar cell. However, the degradation mechanism is found to be significantly slower than under bifacial stress.[35]

Since it is highly unlikely that an electrical field applied at the rear side of the laminate influences positive charges at the front side of the solar cell, additional tests including laminates composed with a transparent frontsheet foil (configuration B) were conducted to clarify this behaviour.

C. Rear-side PID stress in Configuration B samples

Until now we have shown that FJ bifacial solar cells in a glass/glass packaging under rear-side monofacial PID stress exhibit the same degradation behaviour as under bifacial PID stress. Only the degradation rate was found to be lower compared to experiments under bifacial PID stress. To further investigate this behaviour, two identical laminates in configuration B underwent monofacial (rear-side) PID stress testing to investigate the impact of PID on the rear sides of their solar cell separately. This setup is shown in Figure 1c. Since it has been shown in the literature that PID can be avoided by using a transparent backsheet/frontsheet, no degradation due to PID is expected at this side of the solar cell unless the degradation mechanism under rear-side monofacial PID appears to be the same as under bifacial PID stress.[22]

The light I-V curves under front- and rear-side illumination measurements of the first laminate in configuration B during rear-side monofacial PID stress are shown in Figure 6a. Indeed, the results are very clear: over 130 hours of PID stress resulted in a negligible P_{MAX} degradation level of 4% and 2% under front-side illumination measurements for sample one and sample two respectively. Also, under rear-side illumination measurements, we observed a negligible P_{MAX} degradation of 4% and 3% for both modules. It is noted that the P_{MAX} degradation of both modules was mainly caused by FF losses while the I_{SC} and V_{OC}

For Peer Review

remained unchanged. This indicates that the mechanism involved is not the same as in previous tests and might not be caused by the high voltage but rather by the elevated temperature during PID stress.

The EQE measurements under front- and rear-side illumination of the first laminate in configuration B before and after rear-side monofacial PID stress are shown in Figure 6b. In contrast to rear-side monofacial PID stress of laminates in configuration A, no significant change in EQE response has been observed.

D. Rear-side PID stress in configuration A samples with the front side shielded

The previous sections show that bifacial solar cells in a GG configuration under monofacial PID stress unexpectedly degrade at the non-stressed side of the solar cell. As demonstrated, this problem can be solved by replacing the SLG cover with a PID-resistant cover at the non-stressed side. However, it indicates that an unintended electric field arises over the device stack at the side which should not be PID stressed. Hence, when the unintended electric field at the non-stressed side of the solar cell is cancelled out, no degradation due to PID is expected at this side of the solar cell. This was investigated using two identical laminates in configuration A which underwent monofacial (rear-side) PID stress testing with the front side of the laminate shielded from an external electric field. This setup is shown in Figure 1d. The shielding is acquired by attaching an Al foil to the front side of the laminate and short-circuiting it with the solar cell.

The light I-V curves under front- and rear-side illumination measurements of the first laminate in configuration A before and after rear-side monofacial PID stress with the front side shielded from an external electric field are shown in Figure 7a. Over 130 hours of PID stress yielded no significant power loss for both samples under front- and rear-side illumination measurements.

The EQE measurements under front- and rear-side illumination of the first laminate in configuration A before and after rear-side monofacial PID stress with the front side shielded from an external electric field are shown in Figure 7b. In contrast to rear-side monofacial PID stress of laminates in configuration A without the front shielded from an external electric field, no significant change in EQE response has been observed.

4. Discussion

Light IV and EQE measurements indicate that FJ bifacial n-PERT solar cells in a glass/glass packaging (configuration A) under rear-side monofacial PID stress show the same final degradation level as observed after bifacial PID stress. The observed degradation is caused by a mechanism evolving at the front side of the solar cell in both cases. While the final degradation level tends to be the same, the degradation rate differs quite significantly for the samples under rear-side monofacial PID stress. It took approximately five times as long to degrade to the same PID level as for the samples under bifacial PID stress. However, when a frontsheet/glass configuration was used (configuration B), or when the front side of the solar cell was shielded from an external electric field, a negligible change in P_{MAX} degradation was observed after rear-side monofacial PID stress. This points

For Peer Review

out two things: (i) the mechanism under bifacial PID stress is mainly caused by a mechanism evolving at the front side of the solar cell and (ii) the rear side of the solar cell of laminates in configuration A remains unchanged, both under bifacial and rear-side monofacial PID stress.

An explanation of the unexpected degradation evolving at the front side of the solar cells under rear-side monofacial PID stress in a glass/glass packaging can be found in the test setup. One must keep in mind that the frame at the inside of the climatic chamber (mostly manufactured in stainless steel) is grounded, and therefore an unintended electric field between the solar cell (with a potential at -1000 V) and the grounded inside of the climatic chamber is formed. This is clarified in Figure 8a, which shows a sample in configuration A under rear-side monofacial PID stress in a climatic chamber together with the unintended electric field. Indeed, the potential difference in our case will partly be formed across the air gap between the inside of the climatic chamber and the PV laminate and thus the driving force behind the mechanism at cell level will be less, which results in a lower degradation rate, explaining the observed behaviour.

Three measures can be taken (also separately) to avoid this unintended degradation mechanism:

(i) shorting the non-stressed side of the glass/glass laminate with the solar cell (e.g. by an Al foil) and thus cancelling the unintended electric field across the device stack, as shown in Figure 8b;

(ii) using a floating high voltage source; it should be noted that when multiple PV laminates are stacked on top of each other, an unintended electric field in this case can arise between the Al foil and the solar cell of the PV module on top;

(iii) changing the modules topology, i.e. replacing the glass cover by a PID-resistant cover at the non-stressed side.

5. Conclusions

In this work, we used FJ bifacial n-PERT solar cells to investigate the impact of PID testing methodologies as described in the PID standard IEC TS 62804-1. From our results, it is clear that n-PERT solar cells in a glass/glass packaging under bifacial PID stress suffer from a PID mechanism which is only evolving at the front side of the solar cell. However, when the modules underwent monofacial PID stress testing from the rear side only, a similar but slower behaviour was observed, i.e. the PID mechanism evolves at the front side of the solar cell. By PID stress testing identical solar cells in a frontsheet/glass packaging or with the front side shielded from an external electric field, we have shown that this is not the case. In fact, rear-side monofacial PID stress of such bifacial n-PERT solar cells does not initiate a significant power loss.

The explanation of this misinterpretation in results of bifacial solar cells in a glass/glass packaging undergoing monofacial PID stress can be found in the test setup: it is the result of an unintended electric field arising between the grounded inside of the climatic chamber and the solar cell at a negative potential (in our case -1000 V).

For Peer Review

With this paper we aim to raise awareness of this pitfall while conducting PID stress according to the foil-method as described in IEC TS 62804. Therefore, we included three possible measures which should be considered when monofacial PID stress tests of bifacial PV modules are conducted:

(i) shorting the cell and the non-stressed glass cover side (shielding);

(ii) using a floating high voltage source;

(iii) replacing the glass cover by a PID-resistant cover at the non-stressed side.

ACKNOWLEDGEMENTS

IMEC authors acknowledge contribution in the framework of PVMINDS project (call: H2020-EU.1.3.2). This project has received funding from the European Union's Horizon 2020 research and innovation programme under grant agreement 752117.

For Peer Review

References

1. Masson G., Kaizuka I. (2018) Trends 2018 in Photovoltaics Applications. Report IEA PVPS T1-34:2018, International Energy Agency (IEA) Photovoltaic Power Systems (PVPS) Programme.

2. Green, M.A. (2015) The Passivated Emitter and Rear Cell (PERC): From conception to mass production. *Solar Energy Materials and Solar Cells*, 143, 190–197.

3. Meier, S., Wasmer, S., Fell, A., Wohrle, N., Greulich, J., and Wolf, A. (2018) Efficiency Potential of p-type PERT vs. PERC Solar Cells. *In Proc. of the 2018 IEEE 7th World Conference on Photovoltaic Energy Conversion (WCPEC) (A Joint Conference of 45th IEEE PVSC, 28th PVSEC & 34th EU PVSEC)*, 3578–3583.

4. ITRPV – VDMA (2019) International Technology Roadmap for Photovoltaic (ITRPV): 2018 Results. 10th edition, edited by A. Janik-Hannen (VDMA).

5. Köntges M., Oreski G., Jahn U., Herz M., Hacke P., Weiss K.-A., Razongles G., Paggi M., Parlevliet D., Tanahashi T., French R.H. (2017) Assessment of Photovoltaic Module Failures in the Field. Report IEA-PVPS T13-09:2017, International Energy Agency (IEA) Photovoltaic Power Systems (PVPS) Programme.

6. Monokroussos C., Zhang X.Y., Li M., Chen S., Zhou A., Liu S., Zhu J., Wang N., Lee E., Bonilla Castro J., Herrmann W., Schweiger W., Feng V., Zhang Y., and Zou C. (2018) Additional Requirements for Supplementary Rating and Qualification of Bifacial PV-Modules. *Presented at the 2018 International Energy Storage and Mobile New Energy Exhibition & Conference (SNEC 2018),* Shanghai, China.

7. Jaeckel B., Volberg G., Monokroussos C., Mülhöfer G., and Roth A. (2018) Type Approval and Safety Considerations for Bifacial PV Modules: Requirements for IEC 61215 and IEC 61730. *In Proc. of the 35th European Photovoltaic Solar Energy Conference and Exhibition*, Brussels, Belgium, 2018, 997-1000.

8. Gambogi W.J., Demko M., Felder T., MacMaster S., Yu B-L., Borne A., Hu H., and Pan Z. (2019) Performance and Reliability of Bifacial Modules Using a Transparent Backsheet. *In Proc. of the 36th European Photovoltaic Solar Energy Conference and Exhibition*, Marseille, France, 2019, 1054-1058.

9. Kempe, M.D., Miller, D.C., Zielnik, A., Montiel-Chicharro, D., Zhu, J., and Gottschalg, R. (2017) Survey of Mechanical Durability of PV Backsheets. *In Proc. of the 2017 IEEE 44th Photovoltaic Specialist Conference (PVSC)*, Washington, DC, 2017, 3208-3213.

10. Arihara, K., Koyoshi, R., Ishii, Y., Kadowaki, M., Nakahara, A., Nishikawa, H., Takayama, T., Nishimura, H., Ogawa, K., Chiba, Y., and Masuda, A. (2018) Reliability and long term durability of bifacial photovoltaic modules using transparent backsheet. *Japanese Journal of Applied Physics*, 57 (8S3), 08RG15.

11. Luo, W., Khoo, Y.S., Hacke, P., Naumann, V., Lausch, D., Harvey, S.P., Singh, J.P., Chai, J., Wang, Y., Aberle, A.G., and Ramakrishna, S. (2017) Potential-induced degradation in photovoltaic modules: a critical review. *Energy & Environmental Science*, 10 (1), 43–68.

12. Köntges M., Kurtz S., Packard C., Jahn U., Berger K.A., Kato K., Friesen T., Liu H., Van Iseghem M. (2014) Review of Failures of Photovoltaic Modules. Report IEA PVPS T13-01:2014, International Energy Agency (IEA) Photovoltaic Power Systems (PVPS) Programme.

13. Jahn U., Herz M., Köntges M., Parlevliet D., Paggi M., Tsanakas J.A., Stein J.S., Berger K.A., Ranta S., French R.H., Richter M., Tanahashi T. (2018) Review on Infrared (IR) and Electroluminescence (EL) Imaging for Photovoltaic Field Applications. Report IEA PVPS T13-10:2018, International Energy Agency (IEA) Photovoltaic Power Systems (PVPS) Programme.

14. Berghold, J., Koch, S., Pingel, S., Janke, S., Ukar, A., Grunow, P., and Shioda, T. (2015) PID: From material properties to outdoor performance & quality control counter measures. *Reliability of Photovoltaic Cells, Modules, Components, and Systems Viii*, 9563A.

For Peer Review

15. Huang, J., Li, H., Sun, Y., Wang, H., and Yang, H. (2018) Investigation on Potential-Induced Degradation in a 50 MWp Crystalline Silicon Photovoltaic Power Plant. *International Journal of Photoenergy*, 2018, 1–7.

16. Moser, D., Del Buono, M., Bresciani, W., Veronese, E., Jahn, U., Herz, M., Janknecht, E., Ndrio, E., De Brabandere, K., and Richter, M. (2016) Technical risks in PV projects Report on Technical Risks in PV Project Development and PV Plant Operation. *Solar Bankability Project.*

17. Hoffmann, S., and Koehl, M. (2014) Effect of humidity and temperature on the potential-induced degradation. *Progress in Photovoltaics: Research and Applications*, 22 (2), 173–179.

18. Hacke, P., Spataru, S., Terwilliger, K., Perrin, G., Glick, S., Kurtz, S., and Wohlgemuth, J. (2015) Accelerated Testing and Modeling of Potential-Induced Degradation as a Function of Temperature and Relative Humidity. *IEEE Journal of Photovoltaics, 5 (6), 1549-1553.*

19. Naumann, V., Hagendorf, C., and Ilse, K. (2013) On the Discrepancy between Leakage Currents and Potential-Induced Degradation of Crystalline Silicon Modules. *In Proc. of the 28th European Photovoltaic Solar Energy Conference and Exhibition,* Paris, France, 2013, *2994-2997.*

20. Naumann, V., Lausch, D., Haehnel, A., Bauer, J., Breitenstein, O., Graff, A., Werner, M., Swatek, S., Grosser, S., Bagdahn, J., and Hagendorf, C. (2014) Explanation of potential-induced degradation of the shunting type by Na decoration of stacking faults in Si solar cells. *Solar Energy Materials and Solar Cells*, 120, 383–389.

21. Luo, W., Hacke, P., Terwilliger, K., Liang, T.S., Wang, Y., Ramakrishna, S., Aberle, A.G., and Khoo, Y.S. (2018) Elucidating potential-induced degradation in bifacial PERC silicon photovoltaic modules. *Progress in Photovoltaics: Research and Applications*, 26 (10), 859–867.

22. Carolus, J., Tsanakas, J.A., van der Heide, A., Voroshazi, E., De Ceuninck, W., and Daenen, M. (2019) Physics of potential-induced degradation in bifacial p-PERC solar cells. *Solar Energy Materials and Solar Cells*, 200, 109950.

23. Sporleder, K., Naumann, V., Bauer, J., Richter, S., Hähnel, A., Großer, S., Turek, M., and Hagendorf, C. (2019) Local corrosion of silicon as root cause for potential induced degradation at the rear side of bifacial PERC solar cells. *Phys. Status Solidi RRL, 13*, 1900163.

24. Naumann, V., Hagendorf, C., Grosser, S., Werner, M., and Bagdahn, J. (2012) Micro Structural Root Cause Analysis of Potential Induced Degradation in c-Si Solar Cells, *Energy Procedia*, 27, 1–6.

25. Naumann, V., Breitenstein, O., Bauer, J., and Hagendorf, C. (2017) Search for Microstructural Defects as Nuclei for PID-Shunts in Silicon Solar Cells. *In Proc. of the 2017 IEEE 44th Photovoltaic Specialist Conference (PVSC),* Washington, DC, 2017, 1376-1380.

26. Naumann, V., Lausch, D., Grosser, S., Werner, M., Swatek, S., Hagendorf, C., and Bagdahn, J. (2013) Microstructural Analysis of Crystal Defects Leading to Potential-Induced Degradation (PID) of Si Solar Cells, *Energy Procedia*, 33, 76-83.

27. Carolus, J., De Ceuninck, W., and Daenen, M. (2017) Irreversible damage at high levels of potential-induced degradation on photovoltaic modules: A test campaign. *In Proc. of the 2017 IEEE International Reliability Physics Symposium (IRPS)*, Monterey, California, 2017, 2F-5.1-2F-5.6.

28. Carolus, J., Govaerts, J., Voroshazi, E., De Ceuninck, W., and Daenen, M. (2017) Voltage dependence of potential-induced degradation and recovery on photovoltaic one-cell laminates. *In Proc. of the 33rd European Photovoltaic Solar Energy Conference and Exhibition,* Amsterdam, The Netherlands, 2017, *1402-1407.*

29. Naumann, V., Geppert, T., Großer, S., Wichmann, D., Krokoszinski, H.-J., Werner, M., and Hagendorf, C. (2014) Potential-induced Degradation at Interdigitated Back Contact Solar Cells. *Energy Procedia*, 55, 498–503.

30. Halm, A., Schneider, A., Mihailetchi, V.D., Koduvelikulathu, L.J., Popescu, L.M., Galbiati, G., Chu, H., and Kopecek, R. (2015) Potential-induced degradation for encapsulated n-type IBC solar cells with front floating emitter, *Energy*

For Peer Review

Procedia, 77, 356–363.

31. Swanson, R., Cudzinovic, M., DeCeuster, D., Desai, V., Jürgens, J., Kaminar, N., Mulligan, W., Rodrigues-Barbarosa, L., Rose, D., Smith, D., Terao, A., and Wilson, K. (2005) The surface polarization effect in high-efficiency silicon solar cells. *In Proc. of the 15th PVSEC,* Shanghai, China, 2005, 410-411.

32. Lausch, D., Naumann, V., Graff, A., Hähnel, A., Breitenstein, O., Hagendorf, C., and Bagdahn, J. (2014) Sodium Outdiffusion from Stacking Faults as Root Cause for the Recovery Process of Potential-induced Degradation (PID). *Energy Procedia*, 55, 486–493.

33. Luo, W., Hacke, P., Hsian, S.M., Wang, Y., Aberle, A.G., Ramakrishna, S., and Khoo, Y.S. (2018) Investigation of the Impact of Illumination on the Polarization-Type Potential-Induced Degradation of Crystalline Silicon Photovoltaic Modules. *IEEE Journal of Photovoltaics*, 8 (5), 1168–1173.

34. IEC TS 62804–1:2015: “Photovoltaic (PV) modules-Test methods for the detection of potential-induced degradation-Part 1: Crystalline silicon”, IEC, Geneva.

35. Luo, W., Khoo, Y.S., Singh, J.P., Wong, J.K.C., Wang, Y., Aberle, A.G., and Ramakrishna, S. (2018) Investigation of Potential-Induced Degradation in n-PERT Bifacial Silicon Photovoltaic Modules with a Glass/Glass Structure. *IEEE Journal of Photovoltaics*, 8 (1), 16–22.

36. Hacke, P., Smith, R., Terwilliger, K., Perrin, G., Sekulic, B., and Kurtz, S. (2014) Development of an IEC test for crystalline silicon modules to qualify their resistance to system voltage stress. *Progress in Photovoltaics: Research and Applications*, 22 (7), 775–783.

37. Hacke, P., Terwilliger, K., Smith, R., Glick, S., Pankow, J., Kempe, M., Kurtz, S., Bennett, I., and Kloos, M. (2011) System Voltage Potential- Induced Degradation Mechanisms in PV Modules and Methods for Test Preprint. *In Proc. of the 2011 37th IEEE Photovoltaic Specialists Conference,* Seattle, Washington, 2011, 814-820.

For Peer Review

TABLE 1. The initial η, I_{SC}, V_{OC} and FF of the eight single-cell laminates in this PID experiment under front- and rear-side illumination.

	Sample	*η[%]*	*I_{SC}[mA]*	*V_{OC}[mV]*	*FF[%]*
Front	**A1**	19.7	9496	654	77.4
	A2	19.8	9424	659	75.0
	A3	19.3	9410	653	76.2
	A4	19.0	9288	651	76.4
	A5	19.1	9347	658	75.6
	A6	19.4	9454	661	75.4
	B1	19.5	9265	660	77.4
	B2	19.8	9455	655	77.7
Rear	**A1**	16.8	7987	652	78.4
	A2	16.4	7774	653	78.4
	A3	17.6	8614	649	76.5
	A4	16.7	8210	645	76.9
	A5	17.1	8339	654	76.2
	A6	17.8	8731	655	75.7
	B1	16.0	7585	653	78.5
	B2	16.0	7667	648	78.5

For Peer Review

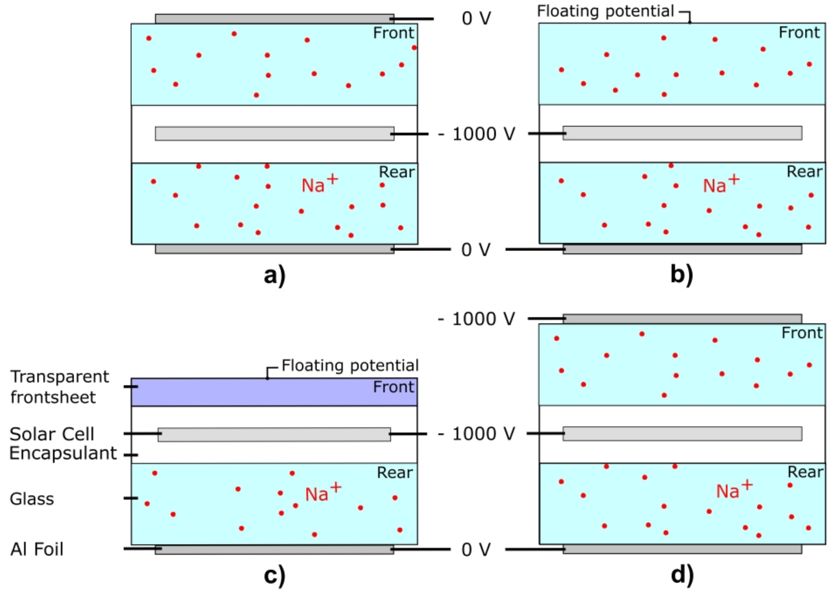

FIGURE 1. Visual representation of the different configurations included in this PID experiment (not drawn to scale). a) laminate in configuration A (glass/glass) undergoing bifacial PID stress, b) laminate in configuration A undergoing rear-side monofacial PID stress while the front side is not shielded, c) laminate in configuration B (frontsheet/glass) undergoing rear-side monofacial PID stress and d) laminate in configuration A undergoing rear-side monofacial PID stress while the front side is shielded. The solar cells were always short-circuited during PID stress.

1250x800mm (600 x 600 DPI)

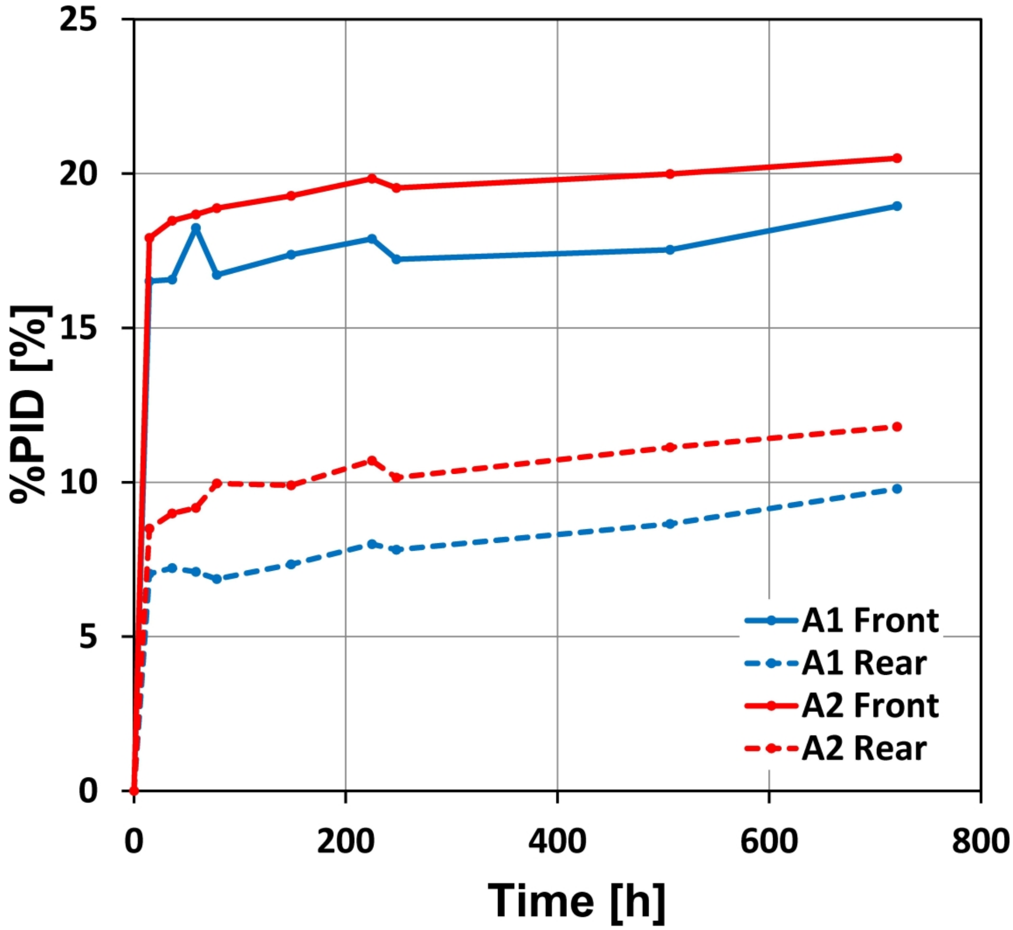

FIGURE 2. The normalized PMAX degradation of the two laminates in configuration A under bifacial PID stress as a function of time.

200x184mm (600 x 600 DPI)

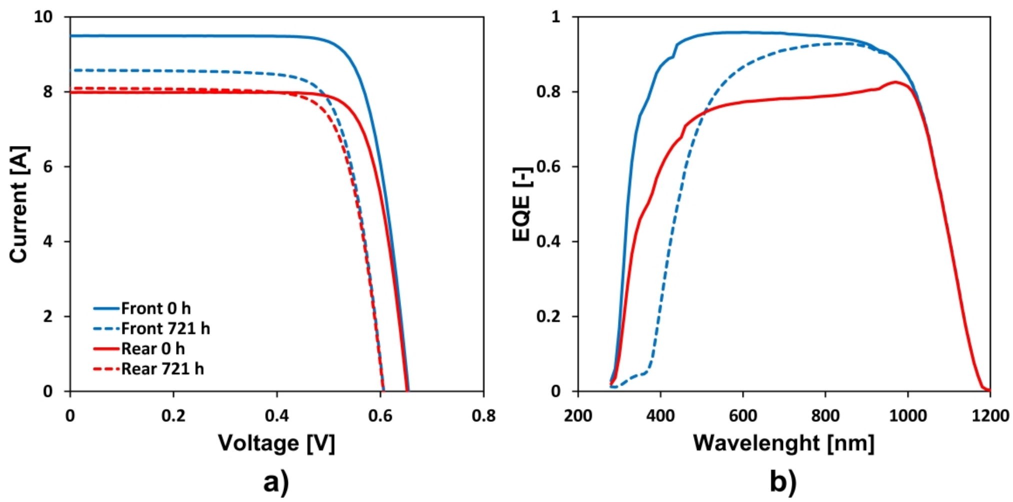

FIGURE 3. a) The I-V curves of the first laminate in configuration A under front and rear-side illumination before and after bifacial PID stress and b) front and rear-side illumination EQE measurements of the same single-cell laminate before and after bifacial PID stress.

373x183mm (600 x 600 DPI)

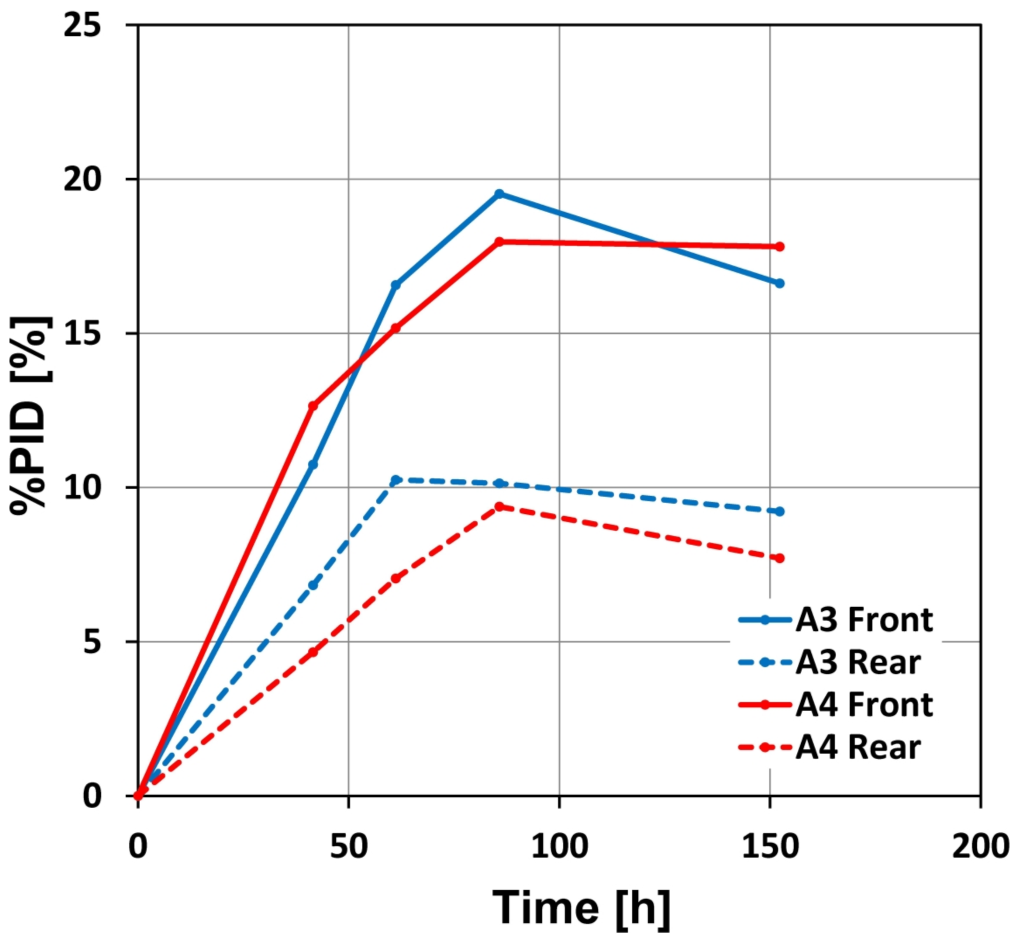

FIGURE 4. The normalized PMAX degradation of the two laminates in configuration A under rear-side monofacial PID stress as a function of time.

200x185mm (600 x 600 DPI)

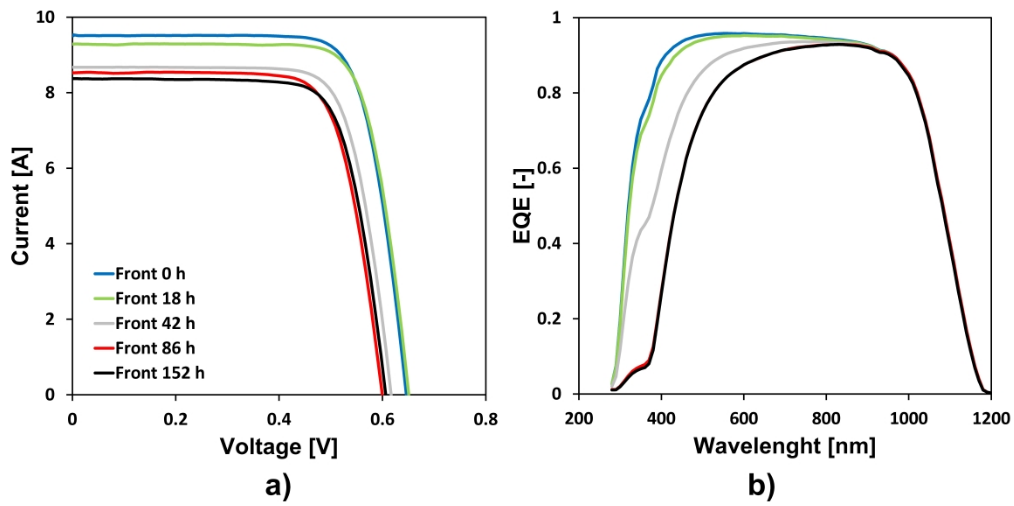

FIGURE 5. a) The I-V curves of the first laminate in configuration A under front side illumination during rear-side monofacial PID stress and b) front-side illumination EQE measurements of the same single-cell laminate during rear-side monofacial PID stress.

372x183mm (600 x 600 DPI)

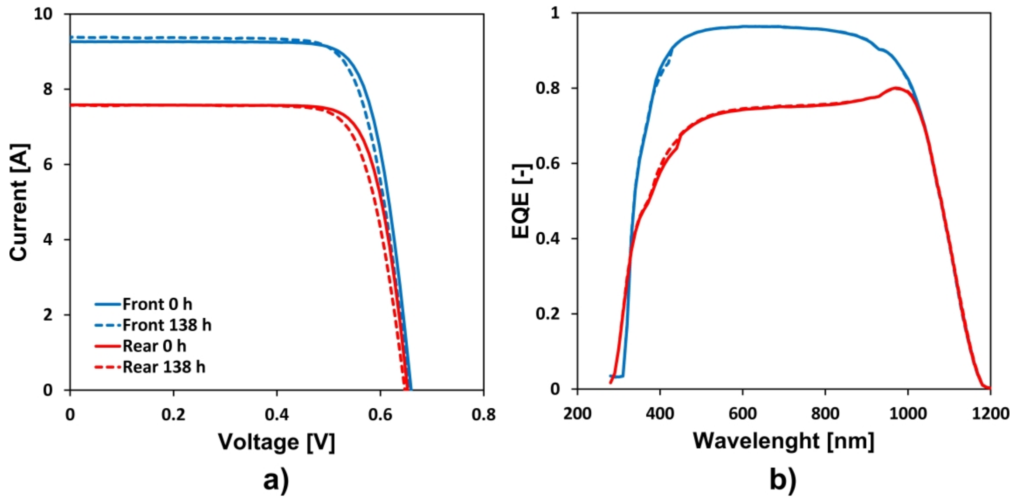

FIGURE 6. a) The I-V curves of the first laminate in configuration B under front and rear-side illumination during rear-side monofacial PID stress and b) front and rear-side illumination EQE measurements of the same single-cell laminate during rear-side monofacial PID stress.

373x183mm (600 x 600 DPI)

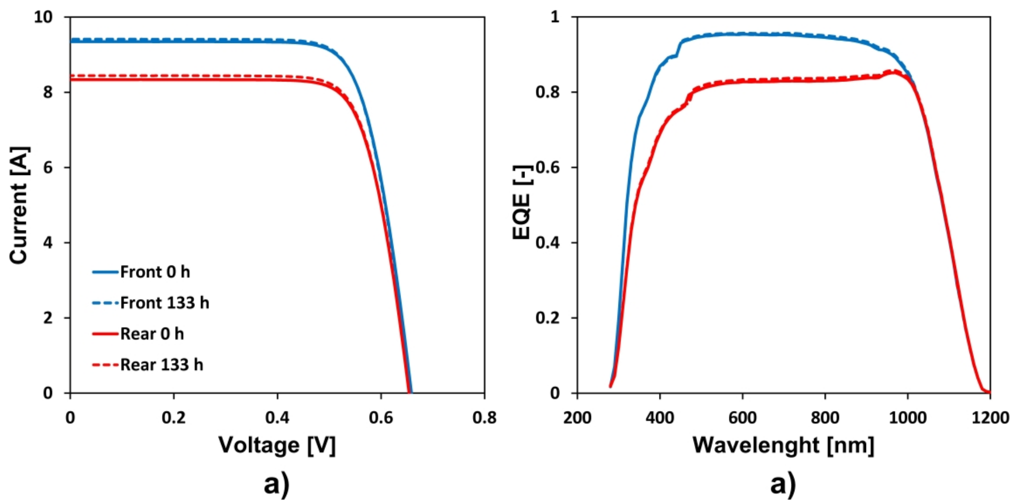

FIGURE 7. a) The I-V curves of the first laminate in configuration A under front and rear-side illumination during rear-side monofacial PID stress while the front side is shielded from an external electric field and b) front and rear-side illumination EQE measurements of the same single-cell laminate during rear-side monofacial PID stress.

373x183mm (600 x 600 DPI)

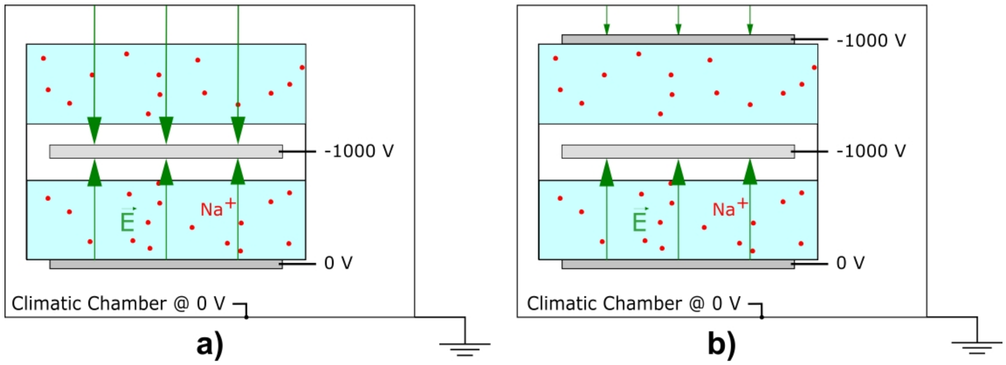

FIGURE 8. A sample in configuration A inside a climatic chamber as included during rear-side monofacial PID experiments without (a) and with (b) shielding the front side of the laminate from an external electric field which arises between the grounded framing of the climatic chamber (at 0 V) and the front side of the solar cell (at -1000 V).

1000x356mm (600 x 600 DPI)